



The impact of climate change on land degradation along with shoreline migration in Ghoramara Island, India

Bijay Halder^{a,*}, Ameen Mohammed Salih Ameen^b, Jatisankar Bandyopadhyay^a,
Khaled Mohamed Khedher^{c,d}, Zaher Mundher Yaseen^{e,f,g,h}

^a Department of Remote Sensing and GIS, Vidyasagar University, Midnapore, 721102, India

^b Department of Water Resources, College of Engineering, University of Baghdad, Baghdad, Iraq

^c Department of Civil Engineering, College of Engineering, King Khalid University, Abha, 61421, Saudi Arabia

^d Department of Civil Engineering, High Institute of Technological Studies, Mrezgua University Campus, Nabeul, 8000, Tunisia

^e Adjunct Research Fellow, USQ's Advanced Data Analytics Research Group, School of Mathematics Physics and Computing, University of Southern Queensland, QLD, 4350, Australia

^f New Era and Development in Civil Engineering Research Group, Scientific Research Center, Al-Ayen University, Thi-Qar, 64001, Iraq

^g College of Creative Design, Asia University, Taichung City, Taiwan

^h Institute for Big Data Analytics and Artificial Intelligence (IBDAAI), Kompleks Al-Khawarizmi, Universiti Teknologi MARA, Shah Alam, 40450, Selangor, Malaysia

ARTICLE INFO

Keywords:

Shoreline change
Land transformation
Coastal development
Remote sensing and GIS
Ghoramara Island

ABSTRACT

Sea level rise (SLR) due to climate change is affecting the coastline, causing shoreline changes, the degradation of mangrove forests, and the destruction of coastal resources. This is the cause of a huge amount of mangrove degradation in many parts of the Ganges–Brahmaputra–Meghna delta. A total of 90% of people have been forced to migrate from the island due to extreme weather conditions. In this study, remote sensing (RS) and geographic information system (GIS) techniques were used for LULC change and shoreline shift analyses of Ghoramara Island. LULC classification was carried out using thirty years of Landsat datasets with intervals of ten years (1990 and 2000) and intervals of five years (2005, 2010, 2015, and 2020). The classification was conducted using a supervised classification method. The field survey data were used to validate the classification results. The total area was reduced from 608 ha (in 1990) to 375 ha (in 2020) due to the extreme weather conditions. Around 39% of the land area was found to be degraded due to shoreline changes. The LULC classes of built-up area, agricultural land, water bodies, and vegetation were found to have lost around 62.345 ha, 63.328 ha, 0.836 ha, and 113.241 ha, respectively, from the year 1990–2020. It was observed that the shoreline shifted towards the north-east, north-west, and southern directions in the last thirty years. This study identified the land use changes due to shoreline shifting and proposed the appropriate to achieve the sustainable development of Ghoramara Island.

1. Introduction

The Sundarban delta and its adjacent areas are more vulnerable due to the effects of climate change, anthropogenic activities, and extreme weather conditions (Chowdhury et al., 2008). Erosion and accretion are common land dynamic processes that take place in coastal regions, meaning that these areas are rapidly changing (Purkait, 2009). Affective tidal activities, waves, and long-shore ocean currents continuously modify the shape of the shoreline in the Ganges–Brahmaputra–Meghna estuarine delta area. Hydro-geomorphological procedures such as erosion and accretion (deposition) are very much active in this area

(Adarsa et al., 2012; Appeaning Addo, 2015; Bandyopadhyay et al., 2004; Ghosh and Mukhopadhyay, 2016; Raju et al., 2010). For the analysis of accretion and erosional processes, shoreline change estimation and investigation are most important parameters for sustainable coastal development. The shoreline of a coastal area is defined as the edge separating the land and water areas, which fluctuates due to the rise and fall of the tides (Cui and Li, 2011; Plater, 2003). The coastal area is highly significant in terms of natural resource management and biodiversity. The coastal region is very vulnerable and can be damaged by extreme weather conditions and natural dynamic procedures such as waves, tidal effects, wind speed, currents, storm surges, coastal erosion

* Corresponding author.

E-mail addresses: halder06bijay@gmail.com (B. Halder), ameen.mohammed@coeng.uobaghdad.edu.iq (A.M.S. Ameen), jatib@gmail.vidyasagar.ac.in (J. Bandyopadhyay), zaheryaseen88@gmail.com (Z.M. Yaseen).

<https://doi.org/10.1016/j.pce.2022.103135>

Received 10 February 2021; Received in revised form 4 February 2022; Accepted 14 February 2022

Available online 16 February 2022

1474-7065/© 2022 Elsevier Ltd. All rights reserved.

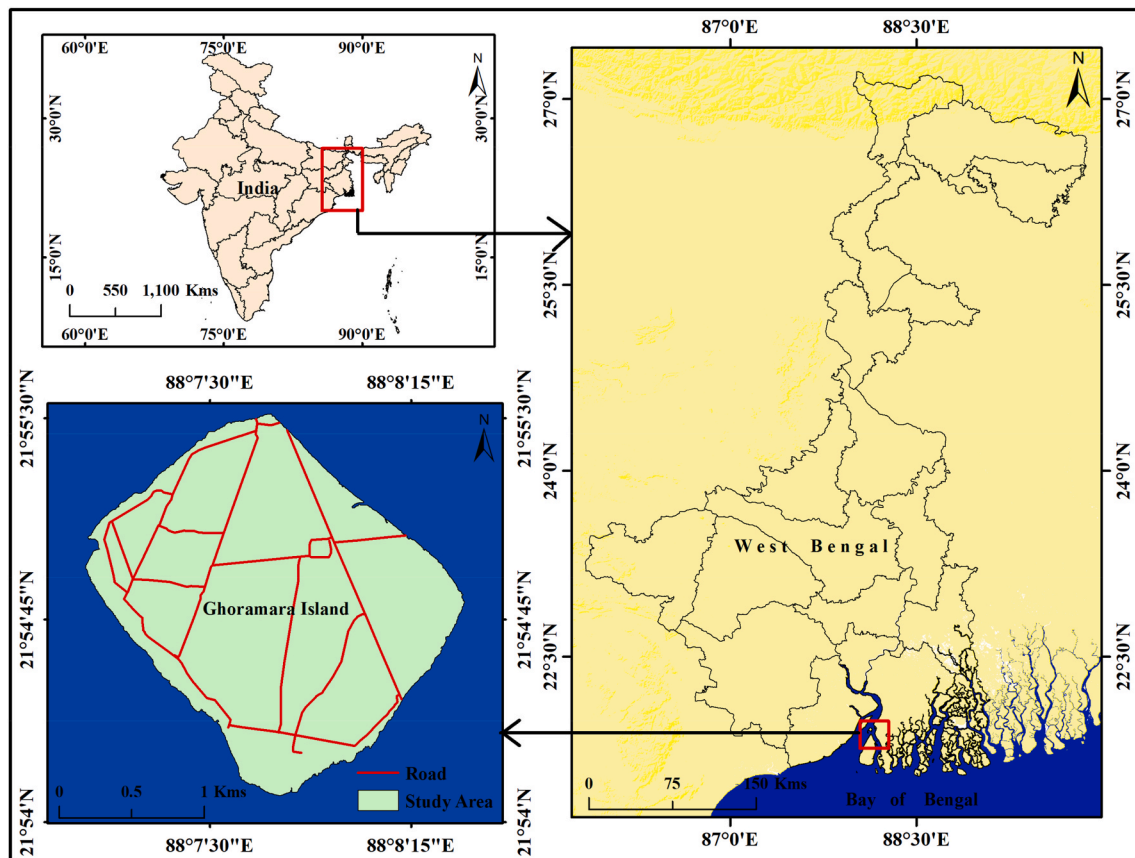


Fig. 1. The location map of the investigated case study area.

and accretion, cyclonic activity, and sediment deposition and transformation (Armanuos et al., 2020; Tao et al., 2021). Anthropogenic activities such as deforestation are also affecting the coastal regions and may cause shoreline shifting over short and long periods (Ghosh et al., 2015). Shoreline change is a major issue affecting the coastal region and is the most important parameter that must be taken into account in future disaster management and planning to protect this area (Mujabar and Chandrasekar, 2011). Due to sea level rise, coastal regions are changing rapidly, damaging the coastal ecosystem and also causing land degradation in some areas. Forest protection is essential for biodiversity conservation and maintaining a sustainable ecosystem (Rodrigues et al., 2021). Forest resources such as food, fodder, fuel, fiber, wood, fruits, tree leaves and eco-tourism are dependent on coastal environmental disturbances, because extreme weather conditions and anthropogenic activities are destroying the ecosystem (Böttcher et al., 2021). A healthier natural environment can ensure sustainable development for people living in coastal areas, stabilize climate fluctuations, help to conserve fresh drinking water, mitigate risk for flood-prone areas, reduce river bank erosion and flood inundation, lower the level of soil moisture, and decrease soil erosion (Poortinga et al., 2018).

Coastal vulnerability can be increased by erosion or shoreline shifting, which can be detrimental to local anthropological activities and coastal areas. The identification of coastline changes is vital in order to understand the dynamics and evaluation of coastal areas (Baig et al., 2020) and enable stakeholders to plan better disaster management systems in order to reduce coastal erosion and minimize social losses, loss of life, physical changes, and economic losses (Fuad and Fais D A, 2017). The most vulnerability areas are located where erosion is high rather than accretion, whereas in less vulnerable areas accretion occurs faster than erosion. Land use and land cover transformation is a very significant parameter for the study of global change due to land alteration. This study aims to help decision-makers, ecosystem managers,

and environmental planners with future worldwide communication (Dwivedi et al., 2005; Fan et al., 2007; Zhao et al., 2004). Land use land cover change is the modification of bio-physical changes in the forest and other areas of Earth's surface (Awadh et al., 2022). At present, forest land is converted to farming land, built-up areas, and aquaculture, leading to degradation of forest areas (Prakasam, 2010).

Earth observational satellite data are useful for detecting, mapping, and investigating land surface alterations as well as in policy making for the future development of this area (AL-Shammari et al., 2021; Salman et al., 2021). Landsat 5 TM and 8 OLI/TIRS data are widely used for monitoring Earth surface phenomena and are available in digital format for machine learning algorithm pre-processing and analysis (Loveland and Dwyer, 2012). The use of satellite-based RS data to identify Earth surface changes due to extreme environmental conditions and anthropogenic activities is cost- and time-effective and easy (Dai and Khorram, 1999). In economically developing countries, people are highly dependent on agriculture, which can be affected by land transformation (Meshesha et al., 2016). However, few studies regarding LULC changes have been carried out on either a short-term or long-term basis (Klein Goldewijk and Ramankutty, 2004). Accuracy Assessment is the satellite data interpretation technique where monitor the user and producer accuracy of the classified maps. Those results are depended on the actual earth surface alteration. In this study, the changes detection technique was used for monitoring the actual land surface and estimating LULC classes, which was important for the generalization and investigation of our objectives. In moderate-resolution satellite data, mixed pixels are a common phenomenon that can increase the variation in classified maps. The change detection method was used to generalize the estimated LULC classes and the actual Earth surface condition.

Multi-temporal Earth observational satellite datasets were used to identify the land degradation and for shoreline change detection on Ghoramara Island. Satellite data are very useful for coastal

Table 1
Data source and date of acquisition.

SL No.	Satellite	Sensor	Date	Path and Row	Data Source
1	Landsat 4-5	TM	14-11-1990	138, 45	https://earthexplorer.usgs.gov/
2			09-11-2000		
3			07-11-2005		
4			06-02-2010		
5	Landsat 8	OLI/TIRS	19-11-2015		
6			16-11-2020		

management, monitoring, and assessment. A geographical information system-based method was used for the shoreline change analysis. Shoreline prediction, topographic and bathymetric information extraction, and coastal zone identification are some of the most important tasks in coastal management. Ghoramara Island is part of the Sundarban delta complex that has had its land area reduced due to embankment failure. This island is located in Hoogly estuary, where salt water mixes with fresh water from the major three rivers in India—i.e., the Ganges, the Brahmaputra, and the Meghna. The present study aimed to identify the land use and land cover changes along with land degradation over Ghoramara Island for South 24 Parganas districts using multi-temporal satellite images. Landsat 5 TM and 8 OLI/TIRS data were used for this study during the periods of 1990–2020. The aim of this study was also to categorize the shoreline shifts and perform erosion–accretion estimation during those years using geospatial technologies.

2. Materials and methods

2.1. Study area

The Ganges–Brahmaputra–Meghna delta is positioned across three major tectonic plates: the Indian Plate, the Burma Plate, and the Eurasian Plate. Most people are dependent on agricultural production, which is the key source of economic development. Anthropogenic activities and extreme weather conditions are the reasons for coastal vulnerability, forest degradation, flood inundation, and shoreline changes. The study area, Ghoramara Island, is affected by extreme weather conditions such as cyclonic storms and tidal effects, which cause shoreline changes, flood inundation, decreased agricultural productivity, land degradation, and soil salinity. Due to global sea level rise (SLR), the forest land and mangrove areas of the Indian Sundarban are decreasing over time. The incidence of flooding has increased due to shoreline shifting, river bank erosion, and sediment transformation, which all increase the coastal vulnerability of this area. The average elevation of this area is 1–2 m above mean sea level (MSL) (Hait and Behling, 2008; Jenice Aroma and Raimond, 2016).

The total, 102 islands can be found in the Indian Sundarban. Of these, 48 islands are covered by mangrove forest and the other 54 islands are inhabited. Ghoramara is the most vulnerable island of India and is located in the South 24 Parganas district. This island is situated around 4 km away from Kakdwip and 1.91 km from Sagar Island. The actual location of this island is 21° 54' 5''N to 21° 55' 29''N and 88° 7' 2''E to 88° 8' 26''E. Once, Ghoramara Island was home to 40,000 people, but due to land degradation and the vulnerability of this island the population has diminished to only 3000 people (Fig. 1). Most residents migrated to obtain a better livelihood. Cultivation, livestock farming, and fishing are the main occupations of residents of this island.

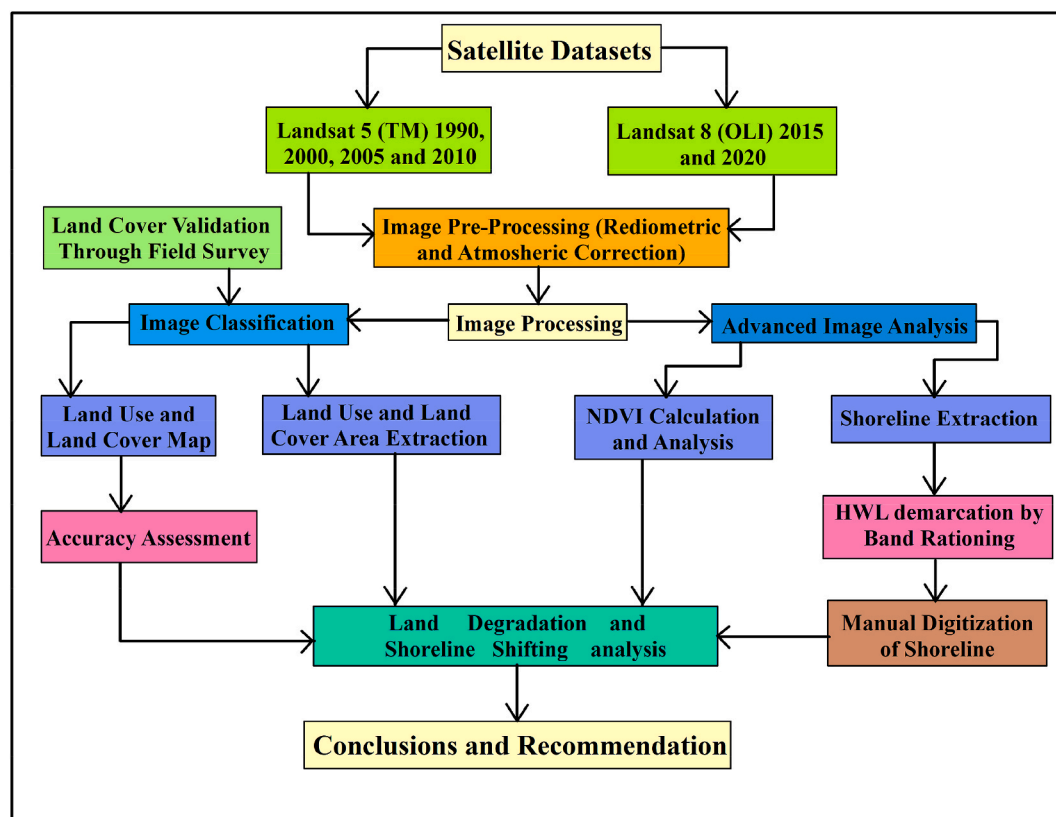


Fig. 2. The overall modeling framework adopted for the current research.

Table 2
Descriptive part of each classified factors of this area.

Sl No.	LULC classes	Description
1	Built-up Area	Residential area, commercial, industrial, transportations, roads and construction area.
2	Vegetation	Area having plantation or natural growing forest, its including many types of trees.
3	Marshy Land	Treeless wetland and mud with distributed grasses.
4	Water Bodies	River, Pond, lakes, and open water area.
5	Agricultural Land	Crop land and fallow land of this area.
6	Sandy Land	Sandy area along with the shoreline

2.2. Data source

Earth observational satellite datasets were used for this study, where the Landsat 5 Thematic Mapper (TM) and Landsat 8 Operational Land Imager/Thermal Infrared Sensor (OLI/TIRS) datasets were derived from the USGS website (<https://earthexplorer.usgs.gov/>). Six temporal datasets were acquired (Table 1) for six different years—i.e., 1990, 2000, 2005, 2010, 2015, and 2020. Table 1 indicates the acquired data and other information of the satellite datasets.

2.3. Image pre-processing

The satellite imagery was pre-processed and geometric correction, atmospheric correction, and topographic correction were carried out in the RS and GIS platform. Pre-processing was conducted before image classification to improve the accuracy and achieve better biophysical singularity. The composite tool from the data management toolbox in ArcGIS 10.5 was used to prepare multiband images, leading to the preparation of false color and/or true color composite images. The satellite datasets were pre-processed in the ERDAS Imagine software v14 for the layer stacking, geo-referencing of the image, masking of the study area, and finally clipping/sub-setting of the study area using Region of Interest (ROI). The satellite images were used for monitoring the Earth surface phenomena and for land transformation estimation using a change detection technique, which was carried out by overlapping of the classified LULC images (Fig. 2).

2.4. Image classification

Earth observational satellite dataset classification was performed by obtaining different categories of the spectral signatures of different temporal Landsat TM and OLI/TIRS imageries. After acquiring the images, band color composite (false color or true color) selection was the most significant factor for the different LULC classes. The NIR and red band were used for monitoring the vegetation area, where the SWIR and NIR bands were used for monitoring the built-up area. Band compositions, such as, short-wave infrared (SWIR), near-infrared (NIR), and red (R) band combinations, were used for the identification of the soil moisture content of build-up areas and bare soil (<https://www.usgs.gov/faqs/>). Each spectral signature was created using polygons in the respective satellite images. A total of 5–45 signatures were taken for each class. An acceptable signature is the one confirming factor that there is ‘minimal confusion’ amongst the land use and land cover to remain planned (Table 2).

Satellite datasets for the different time periods were used for image classification and supervised classification with the maximum likelihood algorithm. Pixel-based image classification is best for land use classification. The likelihood Lk is demarcated as the subsequent possibility of a pixel being appropriate for class k.

$$Lk = \frac{P^k_x = P(k) * P(X_k)}{\sum (i) * P(X_i)} \quad (1)$$

Table 3
Scale of kappa coefficient.

SL No.	Value of K	Strength of agreement
1	<0.20	Poor
2	0.21–0.40	Fair
3	0.41–0.60	Moderate
4	0.61–0.80	Good
5	0.81–1.00	Very good

where P(k) indicates the possibility of detecting X from class k or the possibility concentration purpose (Table 3).

Generally, P (k) are expected to be equivalent to each other and $\sum P(i) * P(x/i)$ indicates the shared class. Therefore, Lk represents the P(X/k) or the possibility concentration purpose (<http://sar.kangwon.ac.kr/etc>).

2.5. Post classification

After classification, a post-classification accuracy assessment is required for monitoring the accuracy of the classification maps (Cheruto et al., 2016). Mixed-pixel data are a common problem for different types of Earth observational satellite datasets with moderate spatial resolution, such as Landsat data (Lu and Weng, 2005). The built-up area is more heterogeneous due to settlement, road, open space, and water bodies, and many urban amenities are located there (Jensen et al., 2007). The visual interpretation of the satellite data is important for classification, and false color composites (FCCs) and true color composites (TCCs) are necessary for image classification. After classification, accuracy assessment and area calculation were carried out using the ArcGIS v10.5 software.

2.6. Accuracy assessment

The accuracy assessment is important for identifying observed and actual Earth surface phenomena. Accuracy assessments are used for monitoring the land use and land cover classification in satellite datasets (Owojori and Xie, 2005). Different year satellite datasets were used to calculate the Earth surface alteration. The accuracy assessment was calculated from the user and producer accuracy of the classification imageries. The omission and commission error due to accuracy assessment was also identified. The ground references, field survey, and Google Earth data were used for monitoring the accuracy. The point-based investigation of the satellite data classification maps and Earth surface actual conditions were correlated and used for identifying the accuracy percentage. The random points were generated and used for estimating the accuracy of the classified maps. This technique is mostly used for monitoring the accuracy of classified maps and investigating changes in the Earth’s surface. If the accuracy is not above an acceptable limit, it may be that the classification maps are improperly classified, or some errors have occurred. After accuracy assessment, kappa coefficient identification is necessary in order to determine the non-parametric classification accuracy.

2.7. Kappa statistic

The kappa coefficient was calculated from the user, producer accuracy, and number of signatures given by the LULC classification. The kappa coefficient was used for confusion matrix assessment, which measured the accuracy of the classified map matrix (Rosenfield and Fitzpatrick-Lins, 1986). The kappa coefficient was calculated from the observed accuracy and expected accuracy of the classification maps and Earth surface phenomena. The kappa coefficient was not only used to calculate the observed and actual scenarios of the Earth surface but also to measure the total disagreement (Cohen, 1968).

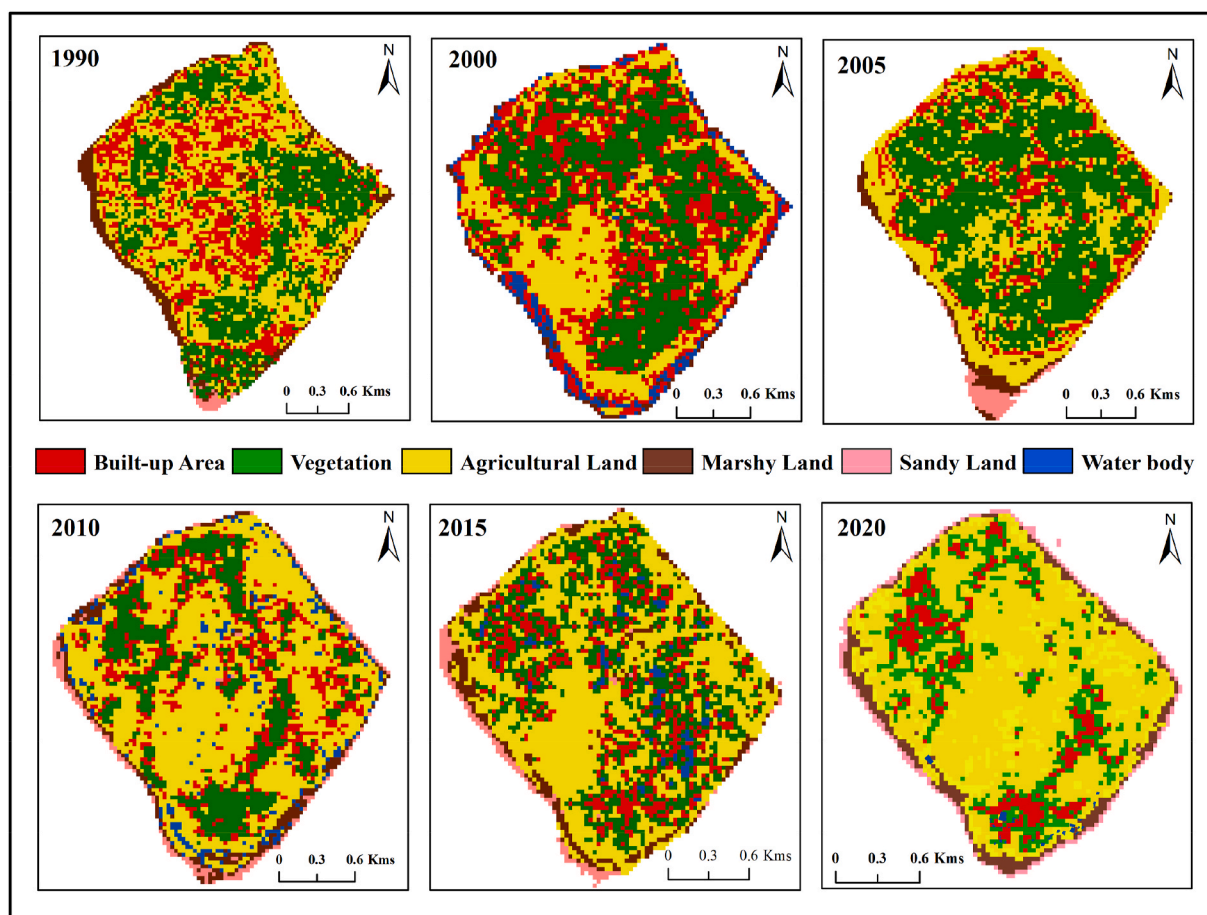


Fig. 3. Land use and land cover map of this study area between 1990 and 2020.

$$K = \frac{(Po - Pe)}{(1 - Pe)} \tag{2}$$

where K means Kappa value, Po represents the observed accuracy, and Pe indicates the chance accuracy. After accuracy assessment, kappa coefficient measurement is necessary for identifying the validity of the LULC classification.

2.8. Shoreline extraction technique

The high water line (HWL) of the satellite datasets was used to identify the actual shoreline shifting of different years of satellite datasets. The HWL has often been used as an identifier (Boak and Turner, 2005) for the highest point of coastal areas or the earlier high tide of the location derived from satellite images and the coast by a noticeable wet/dry strip (Pajak and Leatherman, 2002). The HWL was calculated using band rationing and then digitized in the ArcGIS 10.5 software. Additionally, band rationing was used for estimating the shoreline change of the study area in different time periods. After band rationing, raster to vector analysis is necessary in order to identify the actual shoreline of the study location.

2.9. Normalized difference vegetation index (NDVI)

Forest land is essential for healthier environmental development, because forest area is used to maintain the oxygen balance; decrease the soil salinity and soil erosion; and maintain soil moisture, thermal variation, heat transformation, and infiltration of the groundwater. The surface runoff is also maintained by the forest ecosystem. Many countries have their limits of forest land, with India having 33% forest land.

The overwhelming population pressure, transportation development, deforestation, low afforestation, high level of paper use, and coastal erosion have led to decreases in the area of forests in many parts of the world. Urban expansion is the main reason for forest land losses and thermal variation; extreme weather conditions have also increased mangrove forest area changes. The Normalized Different Vegetation Index (NDVI) is used for monitoring the green space area and in change analysis. Earth observational satellite datasets are used for this type of index-based vegetation monitoring. Landsat TM and OLI/TIRS data with different bands are used for monitoring vegetation changes and the actual scenarios of the Earth surface. The NDVI values vary between -1 and +1, where plus values indicate healthier vegetated land and minus values indicate the open spaces and other LULC classes.

$$NDVI = \frac{NIR - R}{NIR + R} \tag{3}$$

The NIR band indicates the near infrared band and R indicates the red band of the Landsat TM and OLI/TIRS satellite datasets. The given equation indicates the vegetation scenarios because NIR and red bands mostly dominate the green spaces. The NDVI values are also used for the change analysis of the vegetation using high NDVI values and calculating the green space dynamics of the study area.

3. Result and discussion

3.1. Land use pattern of Ghoramara Island

The livelihood of Ghoramara Island mainly depends on its natural resources. Agriculture and fishing (inland and marine) are the main occupations in this area. Due to land degradation, this area has lost a

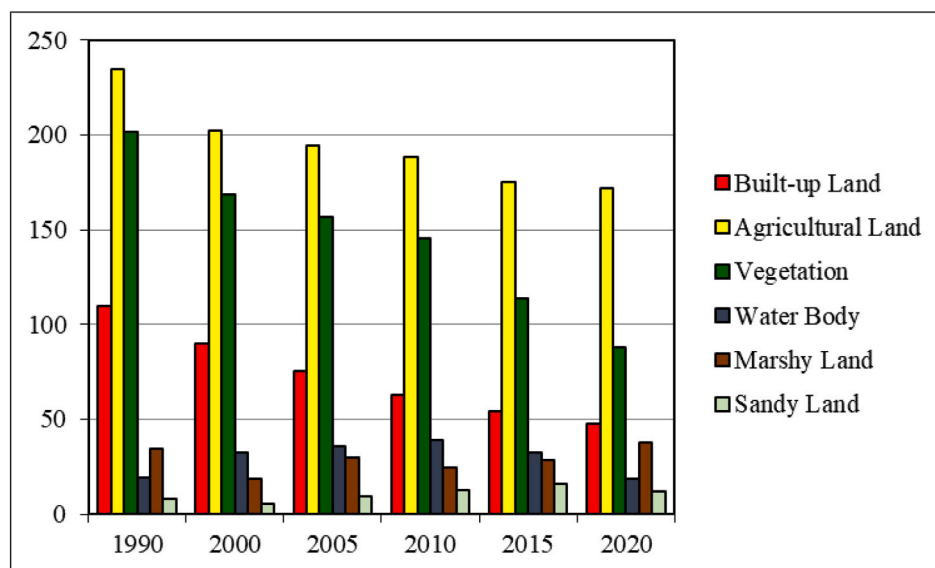


Fig. 4. Area calculation of different land classes of six different years.

huge amount of land in the last thirty years. Land loss is directly affecting the local people, and many of them have migrated to obtain most sustainable livelihoods. However, waterways are the main form of transportation connecting the mainland with this island. In this study, six major land areas were identified: built-up area, vegetation, water-bodies, agricultural land, marshy land, and sandy land. Agricultural activity is the main land use type in this area because the fertile land is used for rice cultivation. Due to shoreline shift, Ghoramara Island has lost its agricultural land and fisheries, which were the main income sources of this area. The marshy land is frequently submerged by tidal water and the shoreline has gradually eroded. The north, north-eastern, and southern parts of Ghoramara Island are highly vulnerable and have lost a lot of land due to sea level rise.

3.2. Land use change calculation

The RS-based land use and land cover classification images of Ghoramara Island for the years of 1990, 2000, 2005, 2010, 2015, and 2020 are shown in Fig. 3. The agricultural land has increased from 1990 to 2020 because of the high production of crops. Inland fisheries and crop production are the main occupations on Ghoramara Island, but people frequently leave this place for other areas to obtain a better livelihood. Sea level rise is affecting the coastal area and around 39% of the area has been lost in just 30 years (Fig. 3). A huge amount of vegetation area has been lost in the study period. In the years of 1990 and 2000, built-up areas were seen scattered in all of the areas, but if we look at other years such as 2005, 2010, 2015, and 2020, we can see that built-up areas have been lost. Mainly, the people in these areas migrated to Kakdwip, Namkhana, Sagar, and the Pathar Patima block of South 24 Parganas district. In the years from 2010 to 2020, the middle and southern parts of this area were changed into agricultural land. Forest land was degraded and converted to agricultural land in the northern, north-east, and southern parts. This study reveals the loss of built-up land.

3.3. Land use/land cover gain and loss

Thirty years of Landsat data were used to classify this study area. The amount of built-up area was 18.053% in the year of 1990, whereas, due to land degradation, the amount of built-up area is gradually reducing. The built-up area was 17.38%, 15.02%, 13.30%, 12.96%, and 12.65% in the years of 2000, 2005, 2010, 2015, and 2020, respectively. However,

Table 4
Erosion and accretion analysis of Ghoramara Island.

Year	Total Area (Ha)	Erosion (Ha)	Accretion (Ha)	Change (Ha)	Remarks
1990	608	-	-	-	-
1990 to 2000	517	90.24	0.76	-89.48	Erosion
2000 to 2005	501	12	4	-8	Erosion
2005 to 2010	472	28	1	-27	Erosion
2010 to 2015	420	51.125	0.875	-50.25	Erosion
2015 to 2020	375	45	0	-45	Erosion

the built-up area of was reduced around 62.345 ha area from the year 1990–2020. Agricultural land occupied 38.66% of the total area of Ghoramara Island in the year of 1990 and 39.18%, 38.78%, 39.88%, 41.72%, and 45.79% of the area in the years of 2000, 2005, 2010, 2015, and 2020, respectively. It was observed that 63.33 ha of agricultural land were lost from 1990 to 2020. The vegetation area was reduced during the last thirty years because people have converted the scattered forest land into agricultural land for crop production and fish cultivation on Ghoramara Island. Again, 33.12%, 32.56%, 31.31%, 30.82%, 27.11%, and 23.50% of scattered forest area was identified in the years of 1990, 2000, 2005, 2010, 2015, and 2020, respectively. The vegetation areas mainly comprised some planted trees, grassland, and natural greenery. In the last 30 years, around 113.24 ha of vegetation has been lost in Ghoramara Island. Those areas have converted into agricultural land and some parts are built-up land. Water bodies were mainly classified into general ponds and inland fisheries. It was observed that shoreline shifting leads to land loss and a loss of water bodies. Some inland fisheries and general ponds are located in middle and shoreline areas in the year of 2020. A total of 3.17% of the area was occupied in the year of 1990, with 6.22%, 7.11%, 8.21%, 7.67%, and 4.92% (Fig. 4) remaining in the years of 2000, 2005, 2010, 2015, and 2020, respectively (Table 5). Marshy land and sandy land are located along the shoreline area of Ghoramara Island. No Mangrove forest is located on Ghoramara Island. Sea level rise affects people’s livelihoods, and the shifting of the shoreline has reduced the area of Ghoramara Island (Fig. 5). This area requires proper planning and management, otherwise the land area of Ghoramara island will be lost in around 40–50 years.

Table 5
Land use and Land cover changes analysis.

Class Name	1990		2000		2005		2010		2015		2020	
	Area (Ha)	Percentage (%)										
Built-up Land	109.76	18.05	89.86	17.38	75.24	15.02	62.78	13.30	54.46	12.96	47.42	12.65
Agricultural Land	235.05	38.66	202.55	39.18	194.28	38.78	188.25	39.88	175.24	41.72	171.73	45.79
Vegetation	201.36	33.12	168.35	32.56	156.86	31.31	145.46	30.82	113.86	27.11	88.12	23.50
Water Body	19.29	3.17	32.14	6.22	35.62	7.11	38.76	8.21	32.21	7.67	18.45	4.92
Marshy Land	34.65	5.70	18.76	3.63	29.77	5.94	24.35	5.16	28.54	6.80	37.54	10.01
Sandy Land	7.88	1.30	5.34	1.03	9.23	1.84	12.39	2.63	15.68	3.97	11.74	3.13

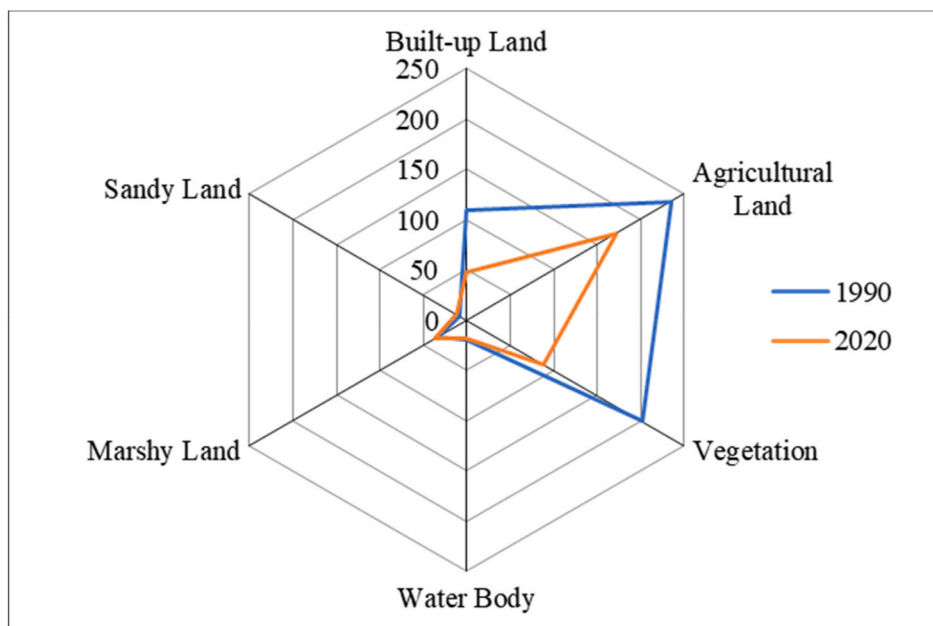


Fig. 5. Spider diagram shows that different land classes in the years of 1990–2020.

Table 6
Confusion matrix of 1990 using Google Earth.

Class Name	Ground Truth/Reference						Row Total	Commission Error	User Accuracy
	Water Body	Built-up Area	Vegetation	Marshy Land	Agricultural Land	Sandy Land			
Water Body	9	1	0	0	0	0	10	10.00%	90.00%
Built-up Area	0	24	2	0	1	0	27	11.11%	88.89%
Vegetation	0	1	28	1	3	0	33	15.15%	84.85%
Marshy Land	1	0	0	10	1	2	14	28.57%	71.43%
Agricultural Land	0	1	5	0	41	1	48	14.58%	85.42%
Sandy Land	0	0	0	2	0	6	8	25.00%	75.00%
Column Total	10	27	35	13	46	9	140		
Omission Error	10.00%	11.11%	20.00%	23.08%	10.87%	33.33%			
Produce Accuracy	90.00%	88.89%	80.00%	76.92%	89.13%	66.67%			
Overall Accuracy	84.29%				Kappa Coefficient	0.7968			

The accuracy assessment and kappa coefficient were calculated in order to validate our classification result (Tables 6–11).

3.4. Assessment of shoreline change

The subsequent changes in the coastline of Ghoramara Island were detected using thirty years of Landsat data following the band rationing method. HWL data were digitized to identify the shoreline of this island. Between the years 1990 and 2020, the shoreline of the entire island shifted north-east; the north-west and southern parts were the most affected by the shoreline shifting. The shoreline was shifted in the north,

north-east, and southern parts of the island and slightly shifted in the south-east and south-west parts from 1990 to 2000. The land area increased from 2000 to 2005; the southern parts accreted but some parts eroded. Between the years of 2010 and 2015, due to sea level rise, the north, north-east, and southern parts were eroded. This same situation occurred during the years 2015–2020 (Fig. 6). Climate change can damage coastal areas and affect the environment (Fig. 7). People have suffered from this land degradation and decrease in Ghoramara Island. In this study, we focused on shoreline shifting due to climate change, which affects the livelihood of people in coastal areas and also leads to land losses. People have lost their cropland and fisheries, and it is now

Table 7
Confusion matrix of 2000 using Google Earth.

Class Name	Ground Truth/Reference						Row Total	Commission Error	User Accuracy
	Water Body	Built-up Area	Vegetation	Marshy Land	Agricultural Land	Sandy Land			
Water Body	10	1	0	1	0	0	12	16.67%	83.33%
Built-up Area	1	28	2	0	1	0	32	6.25%	87.50%
Vegetation	0	4	43	0	5	0	52	17.31%	82.69%
Marshy Land	0	0	2	17	0	1	18	16.67%	94.44%
Agricultural Land	0	1	5	0	48	0	54	11.11%	88.89%
Sandy Land	0	0	0	1	0	6	7	14.29%	85.71%
Column Total	11	34	52	19	54	7	175		
Omission Error	9.09%	17.65%	17.31%	10.53%	11.11%	14.29%			
Produce Accuracy	90.91%	82.35%	82.69%	89.47%	88.89%	85.71%			
Overall Accuracy	86.86%						Kappa Coefficient	0.8279	

Table 8
Confusion matrix of 2005 using Google Earth.

Class Name	Ground Truth/Reference						Row Total	Commission Error	User Accuracy
	Water Body	Built-up Area	Vegetation	Marshy Land	Agricultural Land	Sandy Land			
Water Body	9	0	0	1	0	1	11	18.18%	81.82%
Built-up Area	0	37	2	0	3	0	42	11.90%	88.10%
Vegetation	1	4	49	0	3	0	57	14.04%	85.96%
Marshy Land	1	0	0	11	0	1	13	15.38%	84.62%
Agricultural Land	0	1	3	0	45	0	49	8.16%	91.84%
Sandy Land	0	0	0	2	0	8	10	20.00%	80.00%
Column Total	11	42	54	14	51	10	182		
Omission Error	18.18%	11.90%	9.26%	21.43%	11.76%	20.00%			
Produce Accuracy	81.82%	88.10%	90.74%	78.57%	88.24%	80.00%			
Overall Accuracy	87.36%						Kappa Coefficient	0.8351	

Table 9
Confusion matrix of 2010 using Google Earth.

Class Name	Ground Truth/Reference						Row Total	Commission Error	User Accuracy
	Water Body	Built-up Area	Vegetation	Marshy Land	Agricultural Land	Sandy Land			
Water Body	10	0	0	1	0	2	13	23.08%	76.92%
Built-up Area	0	25	1	0	2	0	28	10.71%	89.29%
Vegetation	0	1	28	0	3	0	31	12.90%	90.32%
Marshy Land	0	0	0	7	0	1	8	12.50%	87.50%
Agricultural Land	1	1	3	0	37	0	42	11.90%	88.10%
Sandy Land	0	0	0	1	0	8	9	11.11%	88.89%
Column Total	11	27	32	9	42	11	131		
Omission Error	9.09%	7.41%	12.50%	22.22%	11.90%	27.27%			
Produce Accuracy	90.91%	92.59%	87.50%	77.78%	88.10%	72.73%			
Overall Accuracy	87.79%						Kappa Coefficient	0.8428	

Table 10
Confusion matrix of 2015 using Google Earth.

Class Name	Ground Truth/Reference						Row Total	Commission Error	User Accuracy
	Water Body	Built-up Area	Vegetation	Marshy Land	Agricultural Land	Sandy Land			
Water Body	4	0	0	1	0	0	5	20.00%	80.00%
Built-up Area	0	21	2	1	4	1	29	27.59%	72.41%
Vegetation	0	1	27	0	4	0	32	15.63%	84.38%
Marshy Land	1	0	0	5	0	1	7	28.57%	71.43%
Agricultural Land	0	1	3	0	21	0	24	16.67%	83.33%
Sandy Land	0	0	0	1	0	2	3	33.33%	66.67%
Column Total	5	23	32	8	29	4	100		
Omission Error	20.00%	8.70%	15.63%	37.50%	27.59%	50.00%			
Produce Accuracy	80.00%	91.30%	84.38%	62.50%	72.41%	50.00%			
Overall Accuracy	80.00%						Kappa Coefficient	0.7340	

difficult to build a sustainable livelihood in Ghoramara Island.

3.5. Erosion and accretion calculation

The delta region is made up of unstable land. The

Ganges–Brahmaputra–Meghna delta is affected by climate change. Sea level rise along with shoreline changes can damage the coastal environment and people's livelihoods. In South 24 Parganas, many islands that have seen recent development have been facing a huge amount of land loss. Ghoramara is one of the islands affected by sea level rise and

Table 11
Confusion matrix of 2020 using Google Earth.

Class Name	Ground Truth/Reference						Row Total	Commission Error	User Accuracy
	Water Body	Built-up Area	Vegetation	Marshy Land	Agricultural Land	Sandy Land			
Water Body	5	0	0	1	0	0	6	16.67%	83.33%
Built-up Area	0	17	2	0	0	0	19	10.53%	89.47%
Vegetation	1	0	23	0	3	0	27	14.81%	85.19%
Marshy Land	0	0	0	4	0	1	5	20.00%	80.00%
Agricultural Land	0	1	5	0	35	0	41	14.63%	85.37%
Sandy Land	0	0	0	0	0	2	2	0.00%	100.00%
Column Total	6	18	30	5	38	3	100		
Omission Error	16.67%	5.56%	23.33%	20.00%	7.89%	33.33%			
Produce Accuracy	83.33%	94.44%	76.67%	80.00%	92.11%	66.67%			
Overall Accuracy	86.00%			Kappa	0.8062				
				Coefficient					

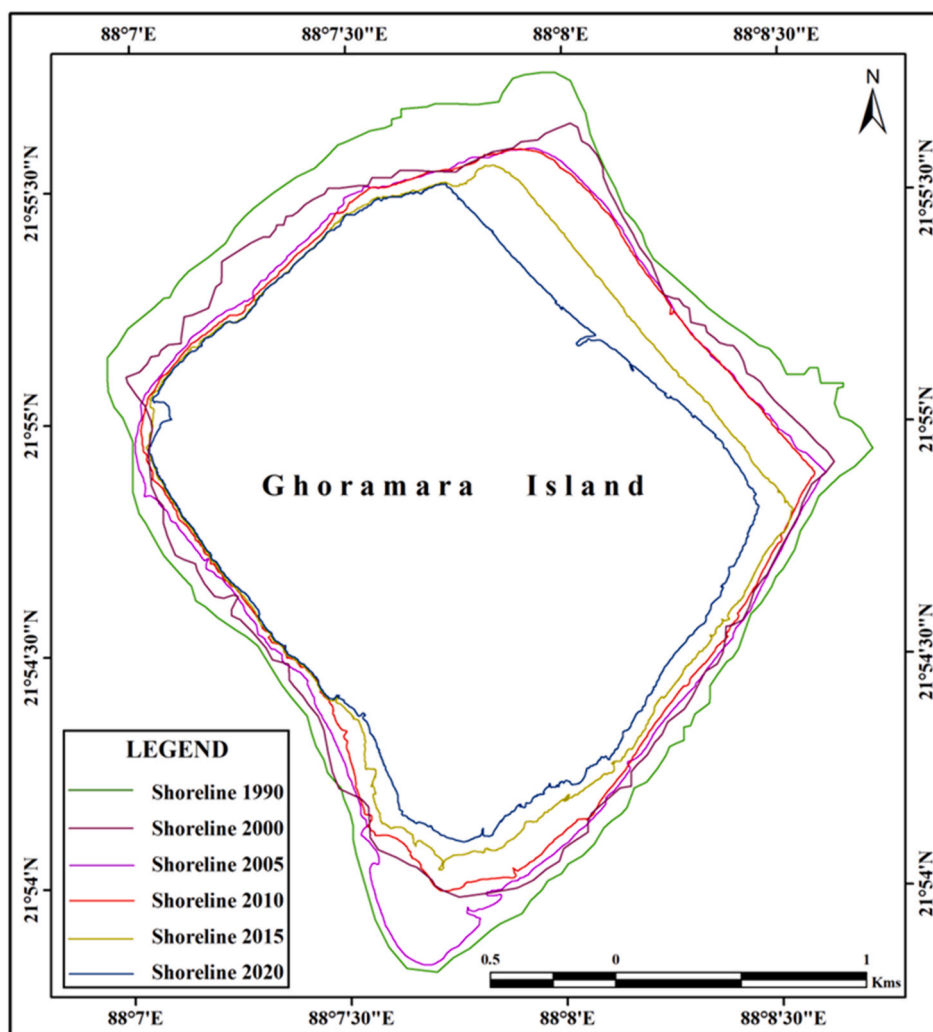


Fig. 6. Shoreline trend map of Ghoramara Island.

has lost a huge amount of its land area. In this study, thirty years (1990–2020) of satellite data were used to identify the shoreline changes. The area of Ghoramara Island in 1990, 2020, 2005, 2010, 2015, and 2020 was 608, 517, 501, 472, 420, and 375 ha, respectively (Fig. 8). Between the years of 1990–2000, an amount of 90.24 ha was eroded while 0.76 ha accreted. Erosion is occurring over time on Ghoramara Island. The population is suffering from this natural disaster and has migrated to other places to obtain a more sustainable livelihood. Between the years of 2000–2005, 2005 to 2010, 2010 to 2015, and 2015

to 2020, amounts of 12, 28, 51.12, and 45 ha of area were eroded (Fig. 9). Agricultural land, built-up land, and many fisheries were destroyed during those periods. Around 39% of the area was eroded in the last thirty years (Table 4). Mangrove forest is a natural barrier that protects coastal regions, but this island does not have any mangrove forest. Planting a mangrove forest is therefore the best option to build a sustainable livelihood on this island.

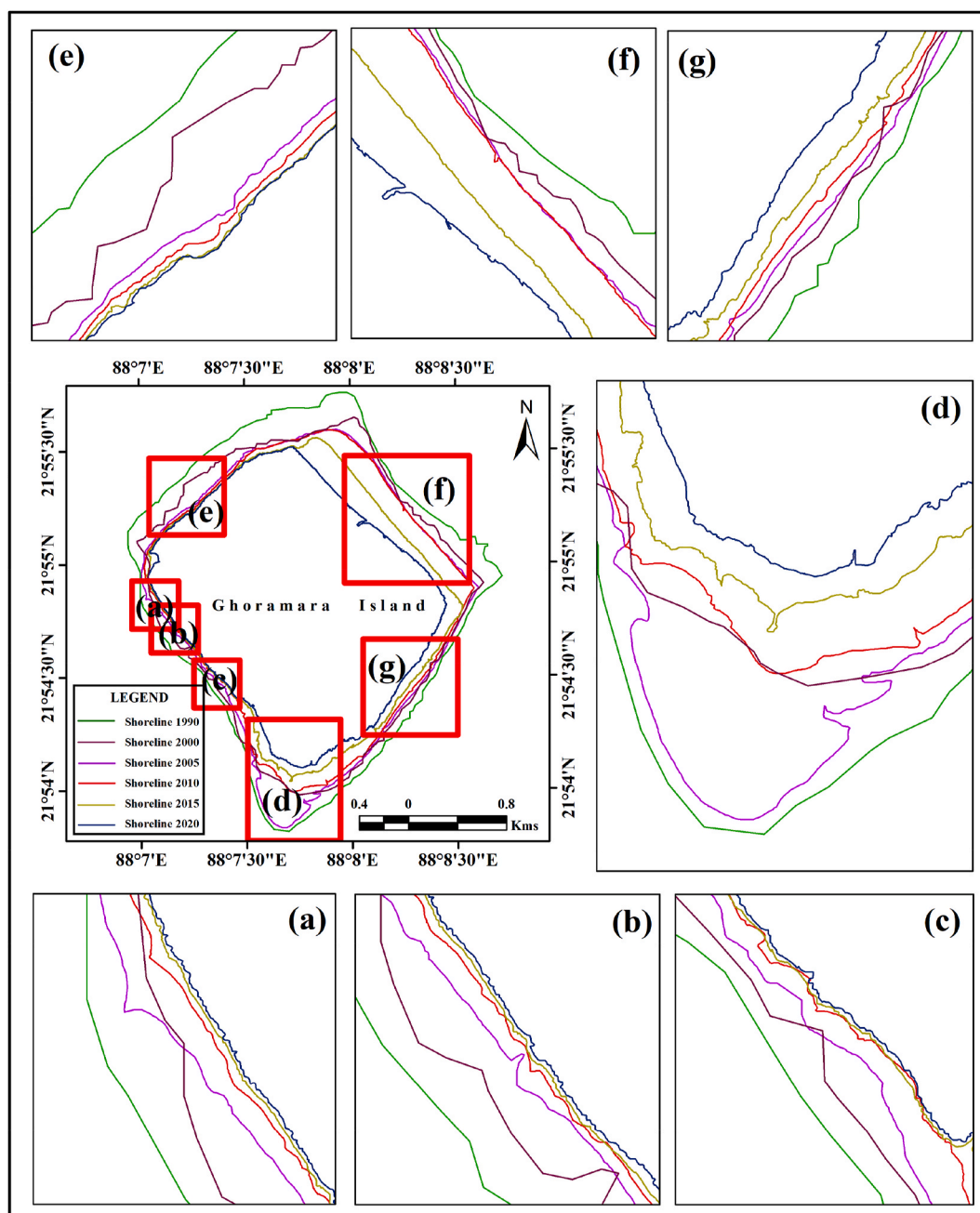


Fig. 7. Shoreline trend of major affected area of this study.

3.6. NDVI investigation

The Normalized Difference Vegetation Index (NDVI) was used to identify the vegetation health of an area. In this study, satellite data from 6 different years were used to calculate the NDVI values. The green color indicates healthy vegetation, whereas the red color on the map indicates lower amounts of vegetation or other LULC classes on Ghoramara Island. The different vegetation index shows that vegetation has decreased due to shoreline changes and saltwater intrusion. Fresh water ponds have been damaged due to land degradation on Ghoramara Island. The highest and lowest values obtained for the year of 1990 were 0.748837 and -0.951219 , respectively (Fig. 10). Similarly, the highest and lowest values obtained for the year 2020 were 0.272969 and -0.0467467 , respectively.

4. Conclusions

The coastal area is very vulnerable to the effects of climate change and changing environmental conditions. Shoreline shifting studies are essential to determine land loss or gain. Shoreline erosion and accretion studies aim to identify means for the sustainable development of the coastal ecosystem and improve people's livelihoods. People who live in coastal areas are suffering hugely from natural disasters such as flooding, land erosion, and saltwater intrusion. In this study, we calculated the land use changes and shoreline shift between the years of 1990 and 2020 for Ghoramara Island, India. Due to population pressure, people can migrate from urban to rural areas and island areas. In recent years (1990–2020), Ghoramara Island has lost around 39% of its land and almost 90% of its people have migrated to other places. The total area of Ghoramara Island in the years of 1990, 2020, 2005, 2010, 2015, and 2020 was 608, 517, 501, 472, 420, and 375 ha, respectively. Most of the

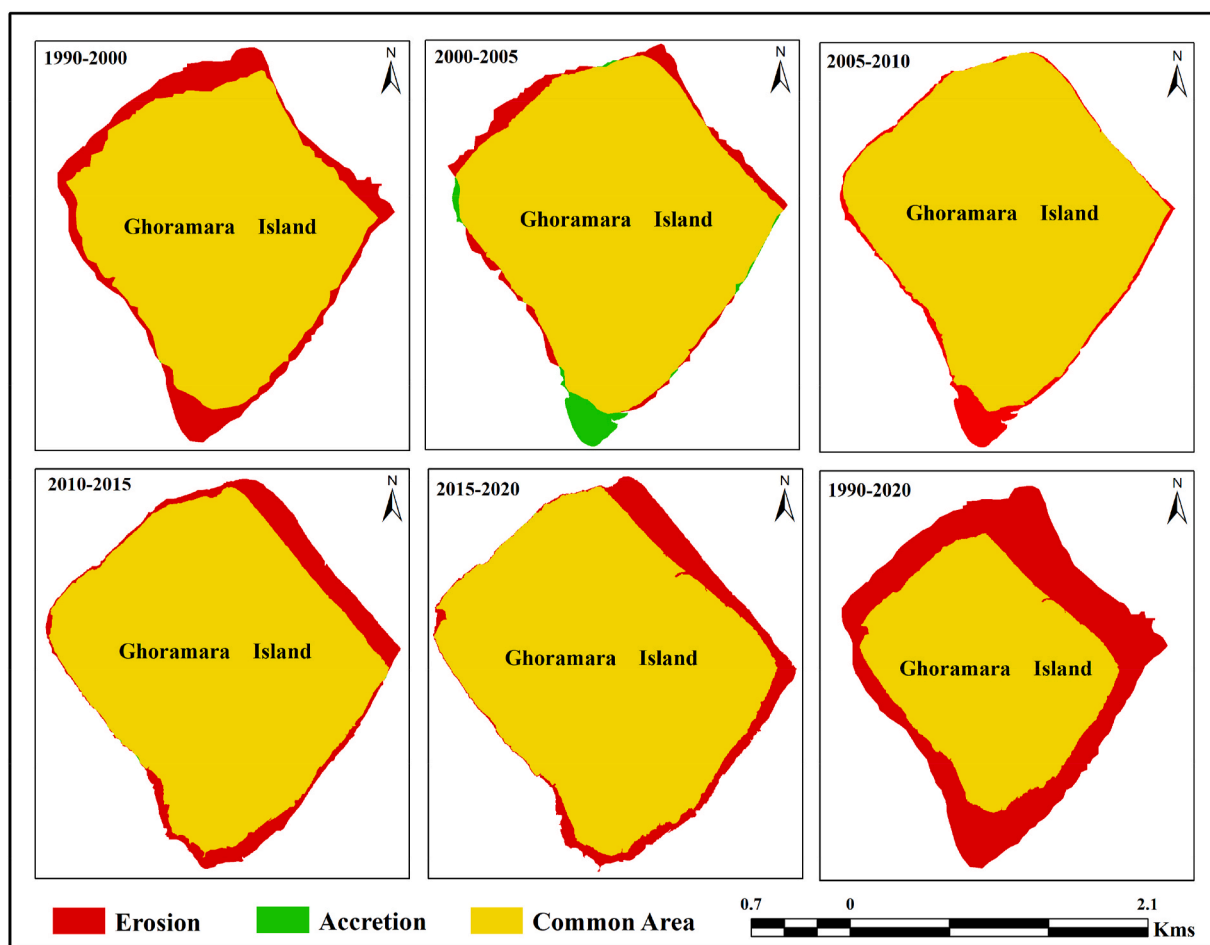


Fig. 8. Erosion and accretion analysis of different years.

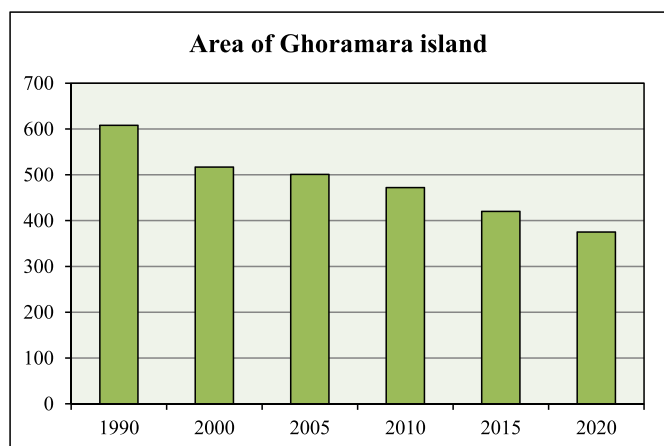


Fig. 9. Total area of Ghoramara Island in different years.

land loss in this area occurred due to climate change. To maintain an equal balance between the natural environment of this area and human intervention, proper attention and management is needed. Otherwise, this island will be quickly eroded in the future and all of its people will be forced to migrate elsewhere. The main problem is that water is the main source connecting it to the mainland. This study aimed to identify the land degradation due to shoreline shifting on Ghoramara Island in order to provide necessary information that would enable appropriate planning for the sustainable management of Ghoramara Island. Further

studies on this topic are needed in order to achieve the better livelihood management of Ghoramara Island with regard to shoreline shifting rate, future shoreline prediction, and socio-economic condition. If we do not pay this topic proper attention, it may create more problems very soon.

Author contribution

Bijay Halder: Conceptualization, project leader, modeling, methodology, investigation, writing up. Ameen Mohammed Salih Ameen: Validation, supervision, validation, technical revision, writing up. Jati-sankar Bandyopadhyay: Conceptualization, supervision, validation, investigation, writing up. Khaled Mohamed Khedher: Conceptualization, supervision, validation, investigation, writing up. Zaher Mundher Yaseen: Validation, supervision, validation, technical revision, writing up.

Funding

This research work was supported by the Deanship of Scientific Research at King Khalid University.

Consistent with the content

The content was helpful for planning and management for sustainable development of Ghoramara Island, West Bengal, India. This content was finding novel results for monitoring the area. 39% of the land was degraded and the result shows that if the situation is same in future, after 40 years the Ghoramara Island will do not situated. Because shoreline change and land degradation will swallow the island.

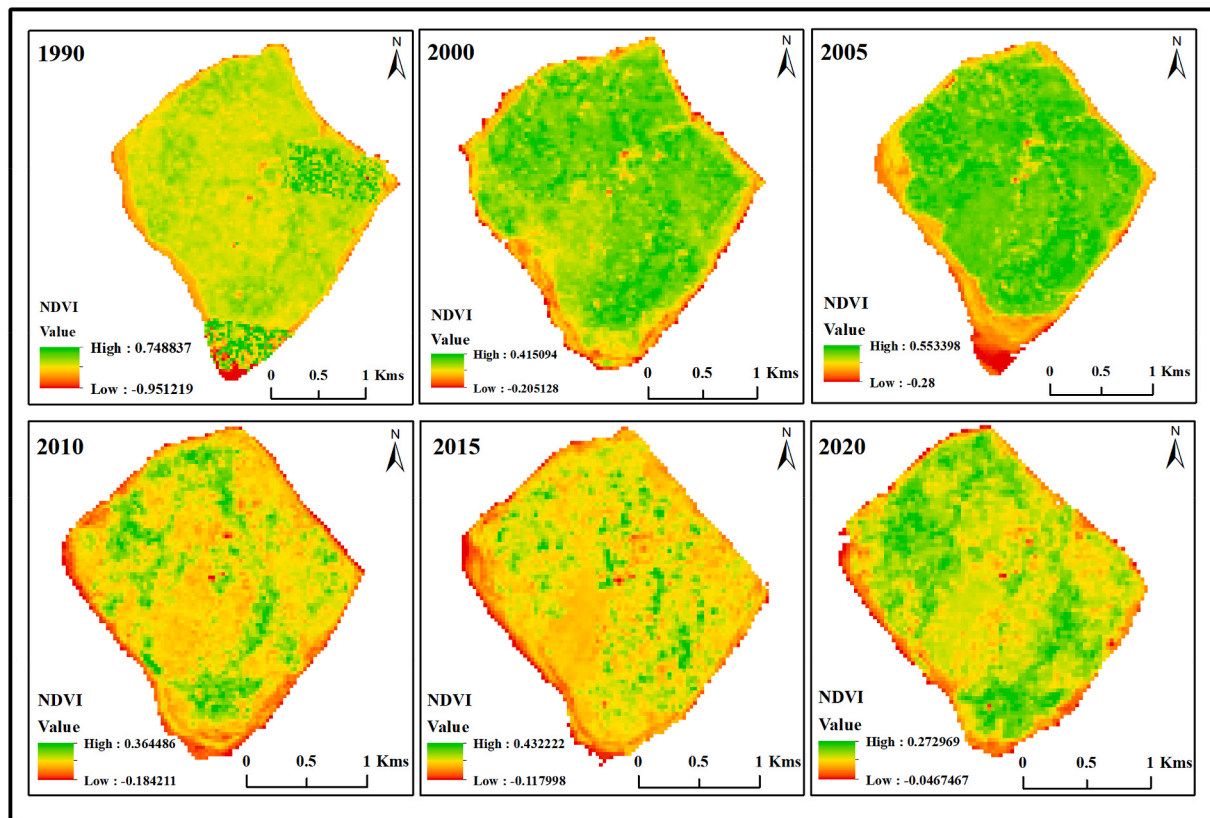


Fig. 10. Vegetation index in different years of Ghoramara Island.

Declaration of competing interest

The authors declare that they have no known competing financial interests or personal relationships that could have appeared to influence the work reported in this paper.

Acknowledge

The Authors extend their thanks to the Deanship of Scientific Research at King Khalid University for funding this work. We are thankful to the Local Government body for our field data collection and other necessary secondary data collection. We also express our gratitude to the United States Geological Survey Department for providing freely satellite data.

References

- Adarsa, J., Shamina, S., Arkoprovo, B., 2012. Morphological Change Study of Ghoramara Island, Eastern India Using Multi Temporal Satellite Data. International Science Congress Association.
- AL-Shammari, M.M.A., AL-Shamma'a, A.M., Al Maliki, A., Hussain, H.M., Yaseen, Z.M., Armanuos, A.M., 2021. Integrated water harvesting and aquifer recharge evaluation methodology based on remote sensing and geographical information system: case study in Iraq. *Nat. Resour. Res.* 1–25.
- Appeaning Addo, K., 2015. Assessment of the volta delta shoreline change. *J. Coast. Zo. Manag.* 18 <https://doi.org/10.4172/2473-3350.1000408>.
- Armanuos, A.M., Al-Ansari, N., Yaseen, Z.M., 2020. Assessing the effectiveness of using recharge wells for controlling the saltwater intrusion in unconfined coastal aquifers with sloping beds: numerical study. *Sustainability* 12, 2685.
- Awadh, S.M., Al-Sulttani, A.H., Yaseen, Z.M., 2022. Temporal dynamic drought interpretation of Sawa Lake: case study located at the Southern Iraqi region. *Nat. Hazards* 1–20.
- Baig, M.R.I., Ahmad, I.A., Shahfahad, Tayyab, M., Rahman, A., 2020. Analysis of shoreline changes in Vishakhapatnam coastal tract of Andhra Pradesh, India: an application of digital shoreline analysis system (DSAS). *Ann. GIS* 26, 361–376. <https://doi.org/10.1080/19475683.2020.1815839>.
- Bandyopadhyay, S., Mukherjee, D., Bag, S., Pal, D.K., Das, R.K., Rudra, K., 2004. 20th century evolution of banks and islands of the Hugli estuary, West Bengal, India: evidences from maps, images and GPS survey. In: Singh, S., Sharma De, H.S., Geomorphol, S.K. (Eds.), *Environ. ACB Publ. Kolkata* 235–263.
- Boak, E.H., Turner, I.L., 2005. Shoreline definition and detection: a review. *J. Coast Res.* 214, 688–703. <https://doi.org/10.2112/03-0071.1>.
- Böttcher, H., Liste, V., Fyson, C., 2021. Options for Multilateral Initiatives to Close the Global 2030 Climate Ambition and Action Gap. Policy field forest protection. Umweltbundesamt (UBA).
- Cheruto, M.C., Kauti, M.K., Kisangau, P.D., Kariuki, P., 2016. Assessment of land use and land cover change using GIS and remote sensing techniques: a case study of makueni county, Kenya. *J. Remote Sens. GIS* 5. <https://doi.org/10.4172/2469-4134.1000175>.
- Chowdhury, A.N., Mondal, R., Brahma, A., Biswas, M.K., 2008. Eco-psychiatry and environmental conservation: study from Sundarban Delta, India. *Environ. Health Insights* 2, EHI-S935.
- Cohen, J., 1968. Weighted kappa: nominal scale agreement provision for scaled disagreement or partial credit. *Psychol. Bull.* 70, 213–220. <https://doi.org/10.1037/h0026256>.
- Cui, B.-L., Li, X.-Y., 2011. Coastline change of the Yellow River estuary and its response to the sediment and runoff (1976–2005). *Geomorphology* 127, 32–40. <https://doi.org/10.1016/j.geomorph.2010.12.001>.
- Dai, X., Khorram, S., 1999. Development of a new automated land cover change detection system from remotely sensed imagery based on artificial neural networks. *IGARSS'97. 1997 IEEE Int. Geosci. Remote Sens. Symp. Proceedings. Remote Sens. - A Sci. Vis. Sustain. Dev.* <https://doi.org/10.1109/igarss.1997.615332>.
- Dwivedi, R.S., Sreenivas, K., Ramana, K.V., 2005. Cover: land-use/land-cover change analysis in part of Ethiopia using Landsat Thematic Mapper data. *Int. J. Rem. Sens.* 26, 1285–1287. <https://doi.org/10.1080/01431160512331337763>.
- Fan, F., Wang, Y., Wang, Z., 2007. Temporal and spatial change detecting (1998–2003) and predicting of land use and land cover in Core corridor of Pearl River Delta (China) by using TM and ETM+ images. *Environ. Monit. Assess.* 137, 127–147. <https://doi.org/10.1007/s10661-007-9734-y>.
- Fuad, M.A.Z., Fais, D.A.M., 2017. Automatic detection of decadal shoreline change on northern coastal of Gresik, east Java – Indonesia. *IOP Conf. Ser. Earth Environ. Sci.* 98, 12001. <https://doi.org/10.1088/1755-1315/98/1/012001>.
- Ghosh, A., Mukhopadhyay, S., 2016. Quantitative study on shoreline changes and Erosion Hazard assessment: case study in Muriganga-Saptamukhi interfluvium, Sundarban, India. *Model. Earth Syst. Environ.* 2 <https://doi.org/10.1007/s40808-016-0130-x>.
- Ghosh, M.K., Kumar, L., Roy, C., 2015. Monitoring the coastline change of Hatiya Island in Bangladesh using remote sensing techniques. *ISPRS J. Photogrammetry Remote Sens.* 101, 137–144. <https://doi.org/10.1016/j.isprsjprs.2014.12.009>.
- Hait, A.K., Behling, H., 2008. Holocene mangrove and coastal environmental changes in the western Ganga-Brahmaputra Delta, India. *Veg. Hist. Archaeobotany* 18, 159–169. <https://doi.org/10.1007/s00334-008-0203-5>.

- Jenice Aroma, R., Raimond, K., 2016. An overview of technological revolution in satellite image analysis. *J. Eng. Sci. Technol. Rev.* 9, 1–5. <https://doi.org/10.25103/jestr.094.01>.
- Jensen, R., Mausel, P., Dias, N., Gonser, R., Yang, C., Everitt, J., Fletcher, R., 2007. Spectral analysis of coastal vegetation and land cover using AISA+ hyperspectral data. *Geocarto Int.* 22, 17–28. <https://doi.org/10.1080/10106040701204354>.
- Klein Goldewijk, K., Ramankutty, N., 2004. Land cover change over the last three centuries due to human activities: the availability of new global data sets. *Geojournal* 61, 335–344. <https://doi.org/10.1007/s10708-004-5050-z>.
- Loveland, T.R., Dwyer, J.L., 2012. Landsat: building a strong future. *Remote Sens. Environ.* 122, 22–29. <https://doi.org/10.1016/j.rse.2011.09.022>.
- Lu, D., Weng, Q., 2005. Urban classification using full spectral information of Landsat ETM+ imagery in marion county, Indiana. *Photogramm. Eng. Rem. Sens.* 71, 1275–1284. <https://doi.org/10.14358/pers.71.11.1275>.
- Meshesha, T.W., Tripathi, S.K., Khare, D., 2016. Analyses of land use and land cover change dynamics using GIS and remote sensing during 1984 and 2015 in the Beressa Watershed Northern Central Highland of Ethiopia. *Model. Earth Syst. Environ.* 2, 1–12. <https://doi.org/10.1007/s40808-016-0233-4>.
- Mujabar, P.S., Chandrasekar, N., 2011. Shoreline change analysis along the coast between Kanyakumari and Tuticorin of India using remote sensing and GIS. *Arabian J. Geosci.* 6, 647–664. <https://doi.org/10.1007/s12517-011-0394-4>.
- Owojori, A., Xie, H., 2005. Landsat image-based LULC changes of San Antonio, Texas using advanced atmospheric correction and object-oriented image analysis approaches. In: *5th International Symposium on Remote Sensing of Urban Areas*. Tempe, AZ.
- Pajak, M.J., Leatherman, S., 2002. The high water line as shoreline indicator. *J. Coast Res.* 329–337.
- Plater, A.J., 2003, 2000. In: Bird, E. (Ed.), *Coastal Geomorphology: an Introduction*, vol. 38. John Wiley and Sons, Chichester, pp. 105–106. <https://doi.org/10.1002/gj.914>, 322 (paperback). ISBN 0 471 89977 1. *Geol. J.*
- Poortinga, A., Clinton, N., Saah, D., Cutter, P., Chishtie, F., Markert, K., Anderson, E., Troy, A., Fenn, M., Tran, L., Bean, B., Nguyen, Q., Bhandari, B., Johnson, G., Towashiraporn, P., 2018. An operational before-after-control-impact (BACI) designed platform for vegetation monitoring at planetary scale. *Rem. Sens.* 10, 760. <https://doi.org/10.3390/rs10050760>.
- Prakasam, C., 2010. Land use and land cover change detection through remote sensing approach: a case study of Kodaikanal taluk, Tamil nadu. *Int. J. Geomatics Geosci.*
- Purkait, B., 2009. Coastal erosion in response to wave dynamics operative in Sagar Island, Sundarban delta, India. *Front. Earth Sci. China*. <https://doi.org/10.1007/s11707-009-0001-0>.
- Raju, D.K., Santosh, K., Chandrasekar, J., Tiong-Sa, T., 2010. Coastline change measurement and generating risk map for the coast using geographic information system. In: *Joint International Conference on Theory, Data Handling and Modelling in GeoSpatial Information Science*. Citeseer, Hong Kong.
- Rodrigues, P., Dorresteijn, I., Guilherme, J.L., Hanspach, J., De Beenhouwer, M., Hylander, K., Bekele, B., Senbeta, F., Fischer, J., Nimmo, D., 2021. Predicting the impacts of human population growth on forest mammals in the highlands of southwestern Ethiopia. *Biol. Conserv.* 256, 109046.
- Rosenfield, G.H., Fitzpatrick-Lins, K., 1986. A coefficient of agreement as a measure of thematic classification accuracy. *Photogramm. Eng. Rem. Sens.*
- Salman, S.A., Shahid, S., Sharafati, A., Ahmed Salem, G.S., Abu Bakar, A., Farooque, A. A., Chung, E.-S., Ahmed, Y.A., Mikhail, B., Yaseen, Z.M., 2021. Projection of agricultural water stress for climate change scenarios: a regional case study of Iraq. *Agriculture* 11, 1288.
- Tao, H., Al-Bedyry, N.K., Khedher, K.M., Shahid, S., Yaseen, Z.M., 2021. River water level prediction in coastal catchment using hybridized relevance vector machine model with improved grasshopper optimization. *J. Hydrol.* 598, 126477.
- Zhao, G.X., Lin, G., Warner, T., 2004. Using Thematic Mapper data for change detection and sustainable use of cultivated land: a case study in the Yellow River delta, China. *Int. J. Rem. Sens.* 25, 2509–2522. <https://doi.org/10.1080/01431160310001619571>.